InP/GaAsSb type-II DHBTs with GaAsSb/InGaAs superlattice-base and GaAsSb bulk-base structures

© Jung-Hui Tsai[¶], Wen-Shiung Lour[*], Der-Feng Guo[×], Wen-Chau Liu[+], Yi-Zhen Wu, Ying-Feng Dai

Department of Electronic Engineering, National Kaohsiung Normal University,
116, Ho-ping 1 st Road, Kaohsiung, Taiwan
[*] Department of Electrical Engineering, National Taiwan Ocean University,
2 Peining Road, Keelung, Taiwan
[×] Department of Electronic Engineering, Air Force Academy, Kaohsiung, Taiwan
[+] Institude of Microelectronics, Department of Electrical Engineering, National Cheng-Kung University,
1 University Road, Tainan, Taiwan

(Получена 27 января 2010 г. Принята к печати 29 января 2010 г.)

High-performance InP/GaAsSb double heterojunction bipolar transistor (DHBT) employing GaAsSb/InGaAs superlattice-base structure is demonstrated and compared with GaAsSb bulk-base structure by two-dimensional simulation analysis. The proposed device exhibits a higher current gain of 257 than the conventional InP/GaAsSb type-II DHBT with a lower current gain of 180, attributed to the tynneling behavior of minority carriers in the GaAsSb/InGaAs superlattice-base region under large forward base−emitter bias. In addition, a larger unity gain cutoff frequency of 19.1 GHz is botained for the superlattice-base device than that of 17.2 GHz for the bulk-base device.

1. Intruduction

Because InP based heterojunction bipolar transistors (HBTs) could provide the devices with several advantages when compared to the GaAs based HBTs, such as 1) lower surface recombination velocity, 2) low electron mass, 3) low turn on voltage, and 4) compatibility with long wavelength photonic devices, they are interesting for a variety of applications, particularly in low-phase-noise oscillator circuits and optoelectronic integrated circuits (OEIC) operating within $1.3-1.5\,\mu$m range [1–3]. However, InP/InGaAs HBTs suffered from low breakdown voltages resulting from the small energy-gap InGaAs collector layer [4,5]. The double heterojunction bipolar transistors (DHBTs) employing a large energy-gap InP or AlInAs material as collector layer could improve the breakdown voltage by reducing impact ionization in the collector layer. Unfortunately, it caused the blocking effect of collector current at base-collector (B−C) heterojunction due to existence of the potential spike [6]. Recently, InP/GaAsSb type-II material system has been as a new alternative for InP-based DHBTs [7,8]. The blocking effect could be completely eliminated, attributed that the conduction band edge of GaAsSb material lays above that of the InP material. Nevertheless, the InP/GaAsSb type-II structure might give rise to the electrons accumulation at B−E junction, which substrantially degrades the current gain [8] (E — emitter).

In this article, the excellent performance of an InP/GaAsSb DHBT with GaAsSb/InGaAs superlattice-base structure is first demonstrated when compared with the GaAsSb bulk-base DHBT. For the superlattice-base DHBT, the current gain can be effectively promoted by tunneling behavior of injecting electrons from emitter into the GaAsSb/InGaAs superlattice-base region.

2. Device structures

The device structure of the studied superlattice-base device (labeled device A) fabricated on an (100)-oriented semi-insulating InP substrate consists of a $0.5\,\mu$m $n^+ = 10^{19}\,\text{cm}^{-3}$ $In_{0.53}Ga_{0.47}As$ subcollector layer, a $0.5\,\mu$m $n^- = 5\times10^{16}\,\text{cm}^{-3}$ InP collector layer, a $p^+ = 4\times10^{19}\,\text{cm}^{-3}$ $GaAs_{0.51}Sb_{0.49}/In_{0.53}Ga_{0.47}As$ superlattice base, a $0.1\,\mu$m $n = 5\times10^{17}\,\text{cm}^{-3}$ InP emitter layer, and a $0.3\,\mu$m $n^+ = 10^{19}\,\text{cm}^{-3}$ $In_{0.53}Ga_{0.47}As$ cap layer. The superlattice base includes ten-period 50 Å $GaAs_{0.51}Sb_{0.49}$ layers and nine-period 50 Å $In_{0.53}Ga_{0.47}As$ layers.

Comparably, the other conventional InP/GaAsSb DHBT (labeled device B) with a 950 Å $p^+ = 4\times10^{19}\,\text{cm}^{-3}$ GaAsSb material as bulk-base layer is proposed to demonstrate the advantage of the studied superlattice-base device.

The concentration and the total thickness in the base region of the two devices are estimated as the same. A two-demensional semiconductor simulation package SILVACO was employed to analyze the energy-band diagrams, carrier distributions, and dc performance [9]. The analysis takes into account the Poisson equation, continuity equation of electrons and holes, Shockley−Read−Hall (SRH) recombination, Auger recombination, and Boltzmann statistics, simultaneously. Fig 1 shows the schematic cross section of the devices A and B. In the devices, the emitter and collector areas are 50×50 and $100\times100\,\mu\text{m}^2$, respectively.

[¶] E-mail: jhtsai@nknucc.nknu.edu.tw

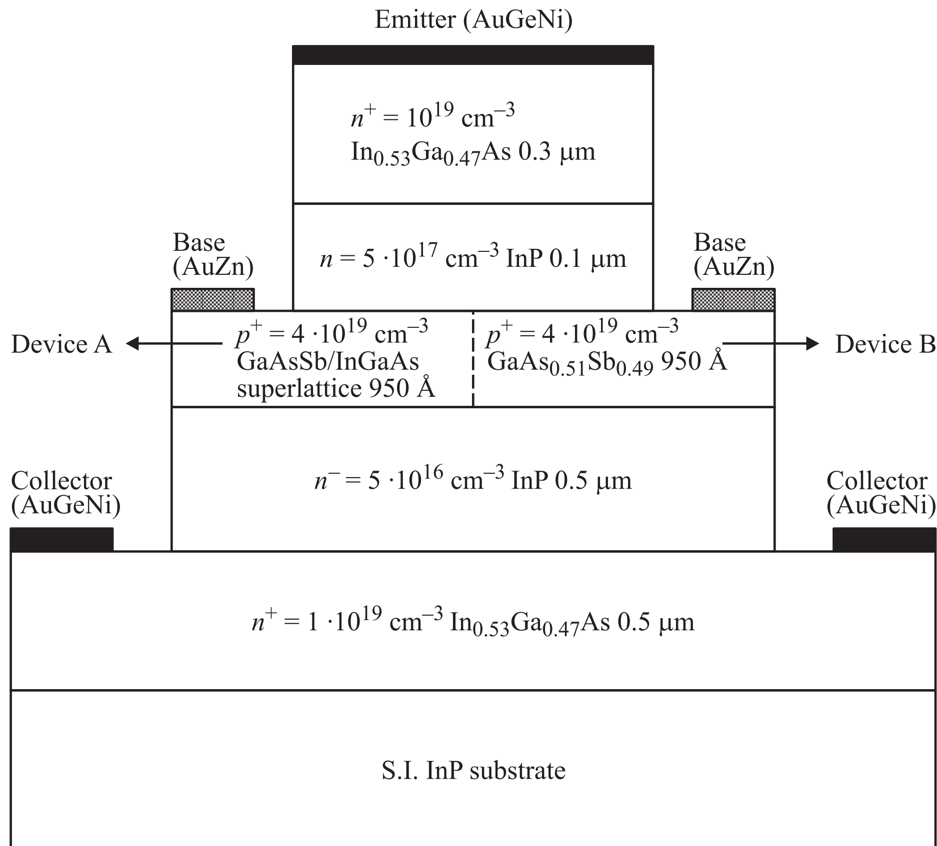

Fig. 1. Schematic cross sections of the studie GaAsSb/InGaAs superlattice-base DHBT (devices A) and GaAsSb bulk-base DHBT (devices B).

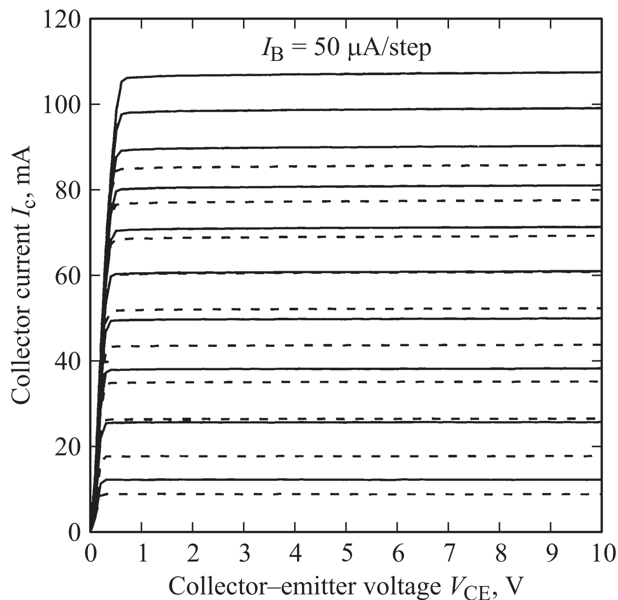

Fig. 2. Common-emitter current–voltage characteristics at room temperature of devices A and B. Solid and dashed lines represent the characteristics of devices A and B, respectively.

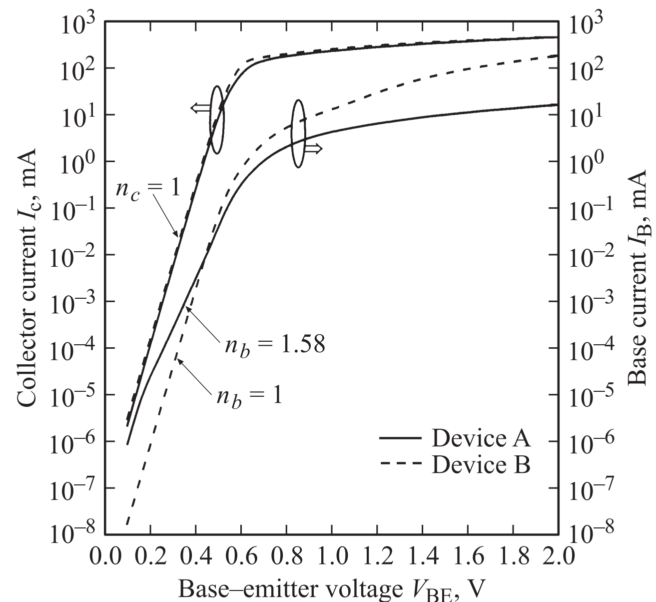

Fig. 3. Gummel plots of the superlattice-base and bulk-base devices at $V_{BC} = 0$.

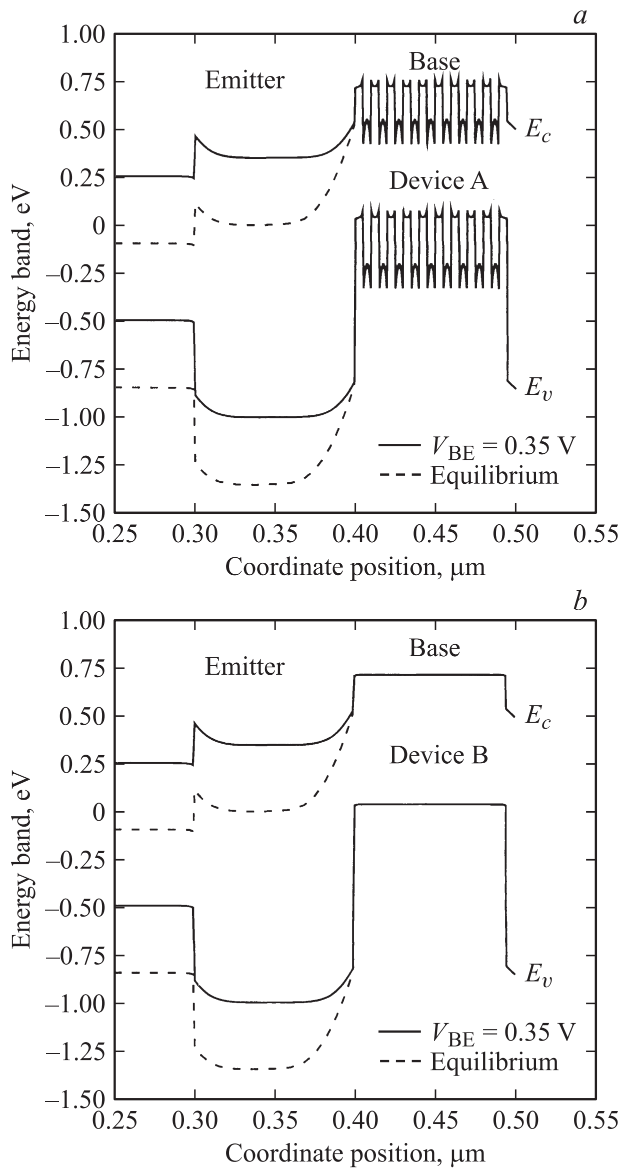

Fig. 4. Energy-band diagrams near the base–emitter junction of (*a*) the superlattice-base DHBT and (*b*) the conventional bulk-base DHBT.

3. Results and discussion

The simulated common-emitter current–voltage ($I-V$) characteristics of the two devices at room temperature are shown in Fig. 2. Clearly, the device A (superlattice-base device) exhibits a higher collector current of 110 mA than that of 87 mA in device B (conventional GaAsSb bulk-base device). In addition, the $I-V$ characteristics of both devices exhibit relatively low collector–emitter offset voltages [10], which implies that the base–emitter (B–E) and B–C junctions are near symmetrical and the employment of superlattice-base structure could not increase the power consumption in circuit application.

Fig. 3 depicts the Gummel plots of the devices at $V_{BC} = 0$. The maximum current gains of 257 and 180 are obtained for the devices A and B, respectively. In both devices, the ideality factor n_C of collector current are nearly equal to unity at low current level, which means that the diffusion mechanism dominates the electron transportation across the B–E junction. Moreover, the collector current I_C of device B is somewhat larger than the device A, because the energy gap of $In_{0.53}Ga_{0.47}As$ ($E_g \approx 0.75$ eV) is slightly larger than the $GaAs_{0.51}Sb_{0.49}$ ($E_g \approx 0.72$ eV) material. On the other hand, at low current level the ideality factors of base current n_b are 1.58 and 1.0 for devices A and B, respectively. The

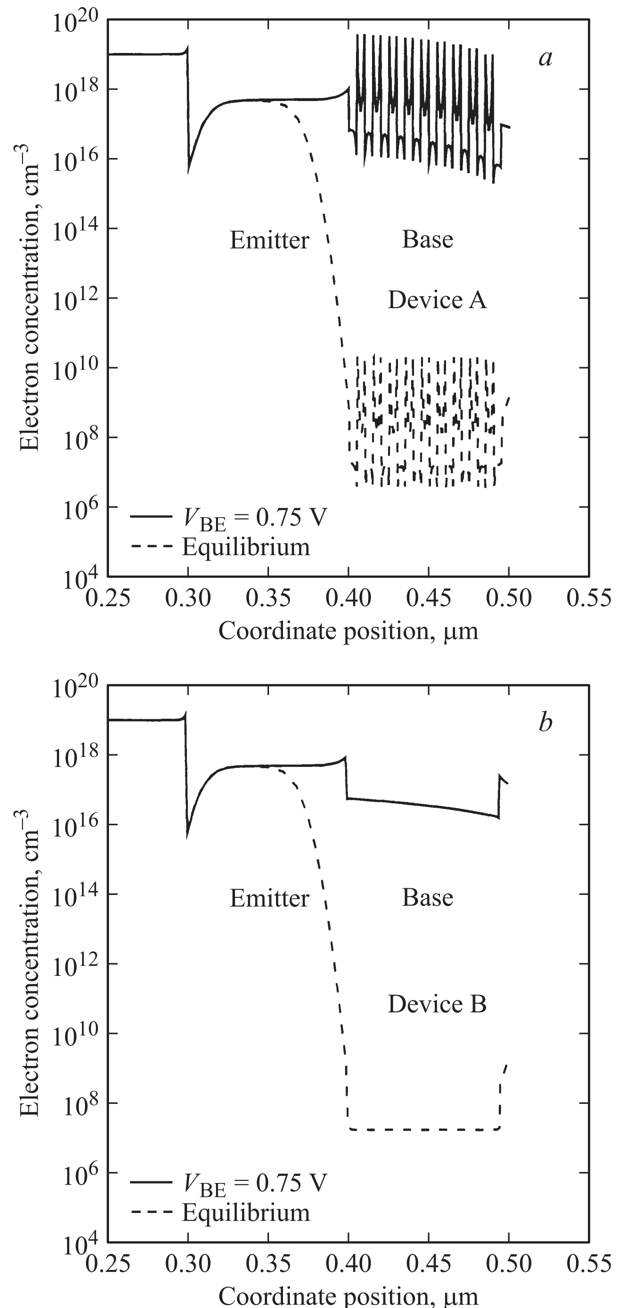

Fig. 5. Electron distributions near the base–emitter junction of (*a*) the superlattice-base DHBT and (*b*) the conventional bulk-base DHBT.

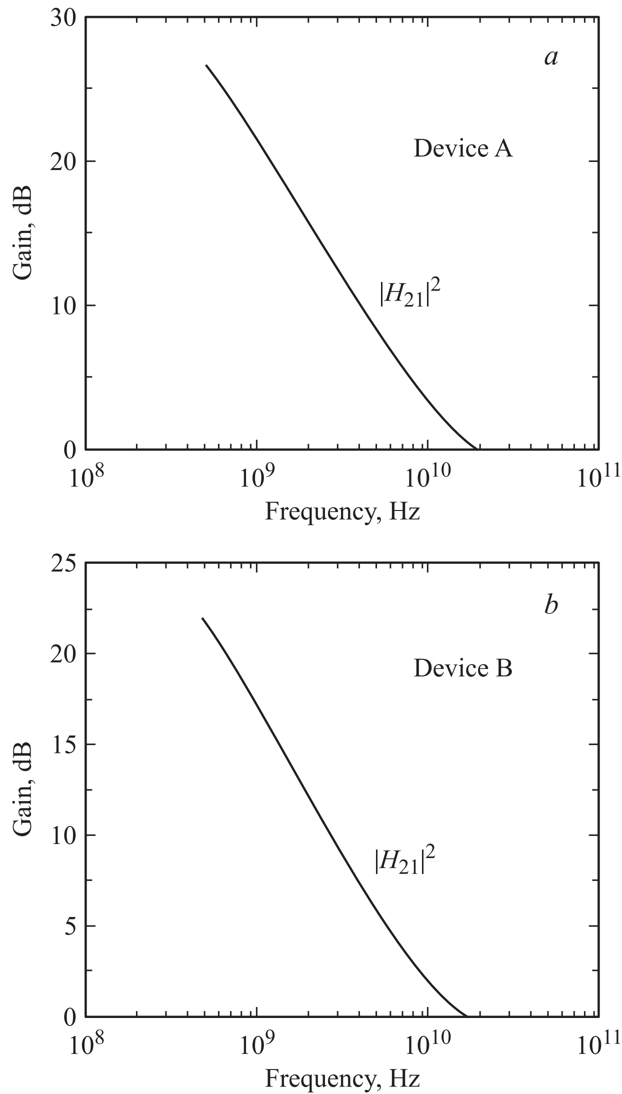

Fig. 6. Ralationship between current gain and operating frequency of (a) the superlattice-base DHBT and (b) the conventional bulk-base DHBT.

device A shows the smaller current gain than the device B under small B–E bias, while it illustrates a greater current gain at $V_{BE} > 0.45$ V. This phenomenon can be explained as follows. We suppose that the base surface recombination current and the B–E depletion-region recombination current are the same for the two devices with similar structures. Then, the hole diffusion curren from base to emitter and the base bulk recombination current might be the main difference in the two devices.

The energy-band diagrams at equilibrium and under forward bias are depicted in Fig. 4. Although the energy-gap difference between $GaAa_{0.51}Sb_{0.49}$ and $In_{0.53}Ga_{0.47}As$ material is relatively small, the valence band of $In_{0.53}Ga_{0.47}As$ material is lower than that of the $GaAa_{0.51}Sb_{0.49}$ material. Thus, for the device A the effective valence band discontinuity (ΔE_v) at B–E junction and the confinement effect for holes will be less that the traditional GaAsSb bulk-base device DHBT under low B–E bias. Furthermore, in this condition some of electrons injecting from emitter region will be partly confined in p^+-$In_{0.53}Ga_{0.47}As$ wells of the superlattice-base region. This will result in large base bulk recombination and base total current, and it trrends to decrease the current gain at small B–E bias. However, it is worthy to note that the superlattice-base device exhibits a larger current gain under large forward bias. Fig. 5 illustrates the electron distributions near the B–E junction of the studied devices. At large B–E voltage, the minority carriers, i. e., electrons, are easy to travel across the superlattice base by tunneling behavior for suppressing the base bulk recombination current as well as total curren and promoting the current gain. In general, the minority carrier (electrons) Q_n in the base region can be given by

$$Q_n = \tau_n J_n(x_p), \quad (1)$$

where τ_n is lifetime of minority carriers, and $J_n(x_p)$ is the electorn current density at the depletion boundary of $p-n$ junction at p-type base side. According to the above equation, the more minority carriers in the superlattice base resulting from the carrier tunneling substantially arises the emitter (and collector) current to increase and the B–E turn-on voltage to decrease. Therefore, the maximum current gain could be substantially improved by the employment of the GaAsSb/InGaAs superlattice-base structure.

The relationship between current gain and operating frequency for the studied devices is depicted in Fig. 6. The current gain curoff frequencies are of 19.1 and 17.2 GHz for the superlattice-base and bulk-base devices, respectively. The smaller the base transient time is, the larger the f_t value is. As compared to the bulk-base device, the tunneling behavior in the superlattice base can decrease the transporting time across the base regime.

4. Conclusion

In summary, the comparison of InP/GaAsSb DHBTs with GaAsSb/InGaAs superlattice-base and GaAsSb bulk-base isinvestigated. Dc current gain and microwave characteristic are improved attributed that the minority carriers are easy to travel across the superlattice-base region by tunneling behavior under large forward B–E bias. Consequently, the proposed superlattice-base device can provide a good potential for signal amplifier and digital circuit applications.

This work is supported by the National Science Council of the Republic of China under Contract No. NSC 98-2221-E-017-012.

References

[1] Y. Matsuoka, E. Sano. Sol. St. Electron., **38**, 1703 (1995).
[2] D. Hadziabdic, T.K. Johansen, V. Krozer, A. Konczykowska, M. Riet, F. Jorge, J. Godin. Electron. Lett., **43**, 153 (2007).

[3] T.P. Chen, S.Y. Cheng, C.W. Hung, K.Y. Chu, L.Y. Chen, T.H. Tsai, W.C. Liu. IEEE Electron. Dev. Lett., **29**, 11 (2008).
[4] K. Ishii, H. Nakajima, H. Nosaka, M. Ida, K. Kurishima, S. Yamahata, T. Enoki, T. Shibata. Electron. Lett., **39**, 911 (2003).
[5] J.H. Tsai, Y.C. Kang. IEEE Trans. Electron. Dev., **53**, 1265 (2006).
[6] H. Wang, G.I. Ng. IEEE Trans. Electron. Dev., **47**, 1125 (2000).
[7] C.R. Bolognesi, M.M. Dvorak, P. Yeo, X.G. Xu, S.P. Watkins. IEEE Trans. Electron. Dev., **48**, 2631 (2001).
[8] Y. Oda, K. Kurishima, N. Watanabe, M. Uchida, T. Kobayashi. *Proc. Int. Conf. Indium Phosphide and Related Mater.* (2006) p. 92.
[9] *SILVACO 2000 Atals User's Manual Editor* I (SILVACO Int. Santa Clara, CA, USA).
[10] J.H. Tsai, W.C. Liu, D.F. Guo, Y.C. Kang, S.Y. Chiu, W.S. Lour. Semiconductors, **42**, 346 (2008).

Редактор Т.А. Полянская